20

Construction of Various Self-assembled Films and Their Application as Lubricant Coatings

Prof. Dr. Jinqing Wang, Dr. Junfei Ou,
Prof. and Dr. Sili Ren and Prof. Shengrong Yang
State Key Laboratory of Solid Lubrication, Lanzhou Institute of Chemical Physics, CAS
P. R. China

1. Introduction

Recently, self-assembled nanofilms (SANFs), including self-assembled monolayers (SAMs), self-assembled multilayer films (SAMFs), self-assembled inorganic films (SAIFs) and self-assembled organic-inorganic composite films (SAO-ICFs), have generated substantial interest not only for its simple preparation procedure but also for its wide potential applications in many fields, such as surface modification, boundary lubricant coatings, sensors, photoelectronics, and functional bio-membrane modeling, etc (Foisner et al., 2004; Gulino et al., 2004; Hsu, 2004; Love et al., 2005; Ostuni et al., 1999; Song et al., 2008; Ulman, 1996; Wang et al., 2005). As a potential lubricant film for controlling stiction and friction in micro-/nano-electromechanical systems (MEMS/NEMS), SANFs offers distinct advantages over other strategies for lubrication of MEMS/NEMS devices. Especially, its assembly process is rapid, shape independent and needs no complicated equipment (Ulman, 1996). In general, the molecules can be assembled onto the targeted surfaces by a simple solution immersion or vapor phase deposition, even within nanoscale crevices between moving components of MEMS/NEMS.

To date, the adhesion, friction and wear behaviors of SANFs are extensively investigated in nanoscale and macroscale by using various techniques and apparatus. Scanning force microscope (SFM) techniques, mainly including atomic force microscope (AFM) (Butt et al., 2005), interfacial force microscope (IFM) (Houston & Michalske, 1992), and chemical force microscope (CFM) (Noy et al., 1997), are often applied to evaluate the nanotribological performances of thin films. In AFM, the adhesive force between the AFM tip and the surface can be calculated from the "force-distance" curve (Cappella & Dietler, 1999) as follows (Tsukruk & Blivnyuk, 1998; Xiao & Qian, 2000):

$$F_{ad} = k_c \times Z_p \times \frac{k_2}{k_1} \tag{1}$$

where k_c is the force constant of the cantilever, Z_p is the vertical displacement of the piezotube, k1 and k2 are the slopes of of the corresponding lines in Fig. 1.

The friction force in nanoscale can also be measured in a contact scanning mode with a scanning angle of 90° or 270° (Fig. 2a). Such scanning will cause torsion of the cantilever and the resultant lateral force is regarded as the friction force (Fig. 2b). Theoretically speaking, the friction force can be easily calculated by applying the Hooke's law:

$$F_{lateral} = k_{lat} \times \frac{\Delta V}{S_{lat}} \tag{2}$$

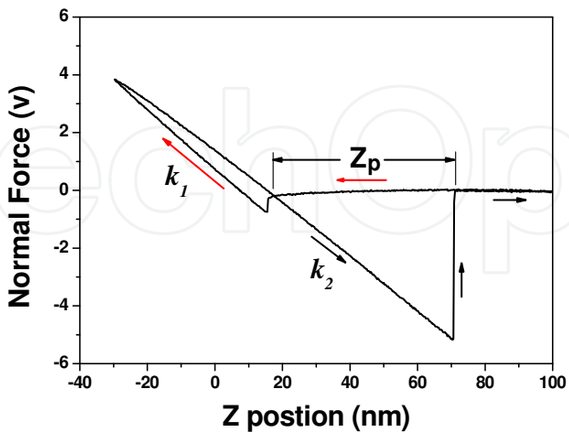

Fig. 1. A typical force-distance curve obtained by AFM.

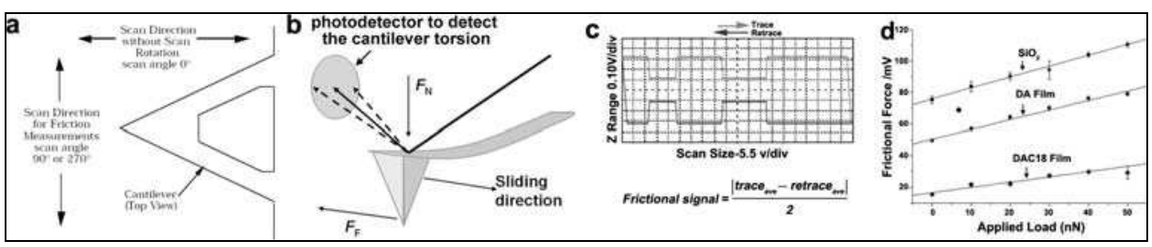

Fig. 2. Scanning angle selection for AFM tip (a); The cantilever torsion at a scanning mode of contact and scanning angle of 90° (b), reproduced from Leggett et al., 2005; A typicaly friction loop (c); Friction versus applied load curves acquired by AFM, reproduced from Song et al., 2008.

where k_{lat} is the lateral spring constant, S_{lat} is the lateral sensitivity of the photodiode, ΔV is the torsion signal. However, the calibration of k_{lat} is still a challenge and therefore the friction force obtained from the friction loops (Fig. 2c) is generally expressed in a raw voltage form in the current studies. By acquiring friction at different applied loads, the friction (F_f)-applied load (F_n) curves can be plotted, which is described by equation (Schwarz et al., 1995):

$$F_f = c_1 F_n^m + c_2 F_n + c_3 \tag{3}$$

where c_1-c_3 are the material-dependent constants and the index m ($0<m<1$) depends on the asperity geometry (Li et al, 1999). However, plenty of studies show that a linear dependence is often observed, equation 3 is therefore simplified to the following form by assuming $c_1 = 0$.,

$$F_f = \mu F_n + F_0 \tag{4}$$

where μ is friction coefficient, and F_0 is assumed to be related with the adhesive force between AFM tip and the surface (Brewer et al., 2001; Foster et al., 2006; Li et al, 1999; Ou et al., 2009; Song et al., 2006; Song et al., 2008; Zhao et al., 2009).

The CFM is distinguished from the usual AFM technique by its probe tip which is chemically immobilized with certain functional molecules (Fig. 3a). This new SFM technique has been used to probe adhesion and friction forces between distinct chemical groups in organic and aqueous solvents. As shown in Fig. 3b, covalent modification of the Si_3N_4 tip with thiols and reactive silanes can be realized by different approaches (Noy et al., 1997).

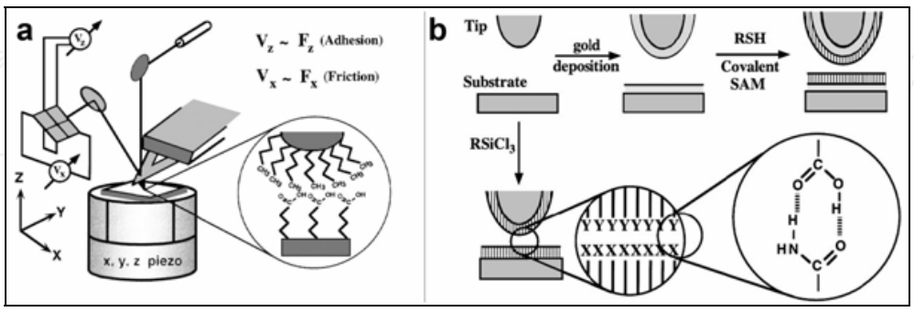

Fig. 3. Schematic drawing of the CFM setup. The inset illustrates the chemically specific interactions between a gold (Au)-coated, CH_3-terminated tip and a COOH-terminated region of a sample (a); Scheme for chemical modification of tips and sample substrates (b). Reproduced from Noy et al., 1997.

Similar to AFM, the IFM is also an ideal tool to investigate the interaction between a scanning tip and a nanoscale surface. The IFM setup is shematically depicted in Fig. 4. As shown in Fig. 4a, a piezo tube acts as a translator to move the mounted sample in *xyz* directions. The probe tip is mounted to a differential capacitor sensor instead of a cantilever in AFM. This special force sensor is mechanically stable and able to determine both the normal and friction forces over the entire range of the interfacial interaction, including the contact and noncontact regions (Fig. 4b, c) (Houston et al., 1992 and 2005).

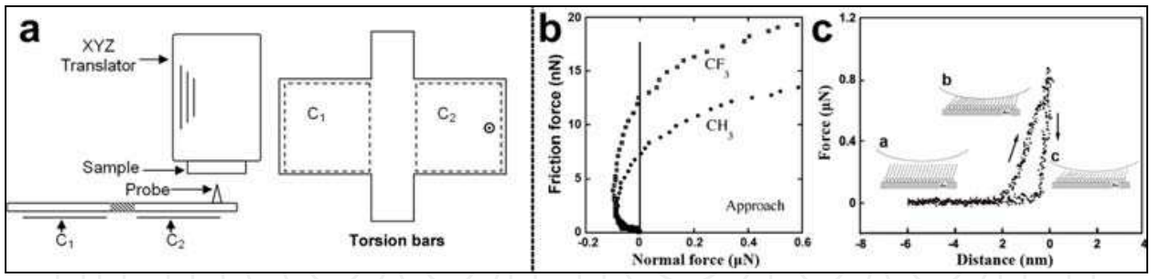

Fig. 4. Schematic of the IFM (a). Averaged IFM data of frictional force vs normal force comparing the behavior of the CH_3- and CF_3-terminated films (b); An interfacial force profile (that is, force versus separation) for a 500 nm radius W probe interacting with an Au sample surface covered by SAMs of n-alkanethiol molecules (c). For b and c, negative values indicate attractive forces while repulsive forces are shown as positive. Reproduced from Houston & Michalske, 1992 (a and c) and Houston et al., 2005 (b).

To investigate the macrotribological behaviors, various ball-on-plate tribometers, such as UMT, are usually applied. The friction coefficient versus sliding time curve of the tested specimen can be recorded automatically as the reciprocating sliding goes on. From this curve, the macroscopic friction coefficient and anti-wear life, which refers to the sliding time at which friction coefficient rises sharply, corresponding to lubrication failure, can be reflected (Fig. 5c).

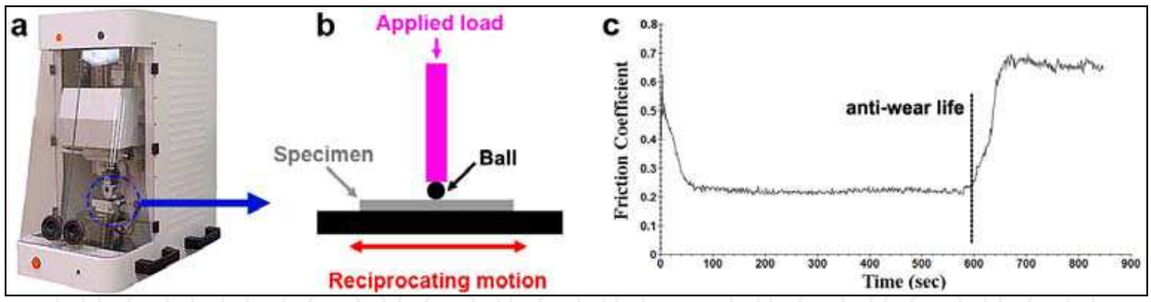

Fig. 5. The photo of a UMT tribometer (a) and the schematic operation principle (b); A friction coefficient versus time curve acquired by a UMT tribometer (c).

As these techniques developed, lots of researches have been done. It is revealed that the tribological properties are structure and composition dependent. Roughly speaking, the alkyl chain length and head/tail group of SAMs have a great influence on its tribological behaviors. For SAMFs, the nature of each layer and the interaction between adjacent layers are key factors. In this chapter, the tribological behaviors of SANFs, including SAMs, SADLs, SAMFs, and SAO-ISFs, are reviewed, aiming at discovering the basic "microstructures-properties" correlation.

2. SAMs

2.1 One component SAMs

SAMs have been widely investigated in the past 20 years because of its potential applications in the field of surface modification, boundary lubricant, sensor, photoelectronics, and functional bio-membrane modeling, etc (Foisner et al., 2004; Gulino et al., 2004; Hsu, 2004; Love et al., 2005; Ostuni et al., 1999; Ulman, 1996; Wang et al., 2005). On the basis of the surface chemical reaction and synthetic approaches, the chemical structures of SAMs can be manipulated easily at molecular level. Generally, two kinds of SAMs, namely, monolayers of alkylsilanes on silicon (Si) wafer surfaces and the monolayers of alkylthiols on Au surfaces (Tsukruk, 2001; Love et al., 2005), have been intensively studied as model lubricants not only for their excellent tribological properties but also for the wide application of Si substrate in MEMS/NEMS and the highly ordered structures of Au wafer. As schematically shown in Fig. 6, the precursor surfactant molecules [X_3Si-$(CH_2)_n$-Y, HS-$(CH_2)_n$-Y, X=-Cl/-OCH_3/–OC_2H_5] of SAMs consist of three parts, viz, head groups (X_3Si- or HS-), alkylchains [-$(CH_2)_n$-], and tail groups (Y). Each part has great effect on the quality and tribological property of SAMs.

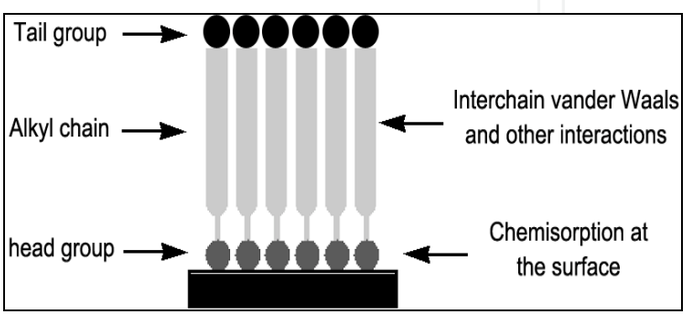

Fig. 6. A schematic view of the formation and forces in a SAMs.

The influence of headgroups

The head groups interact with the active substrate through certain covalent bonding and serve as anchoring points to determine the affinity and stability of SAMs. The superiority of covalent bonding can be reflected by comparing with another popular candidate for MEMS/NEMS lubricant of Langmuir-Blodgett (LB) film, which attaches to the substrate via weak van der Waal force. As expected, SAMs is found to be much more stable against shear stress and possesses better wear resistance as compared with LB film with similar composition and structures (Bliznyuk et al., 1998; Bushan et al., 1995; DePalma & Tillman, 1989; Kim et al., 1999; Overney et al., 1992; Peach et al., 1996; b,Tsukruk et al., 1996; Tsukruk, 2001.). As shown in Fig. 7, C18 SAMs possess much better wear resistance as compared with zinc arachidate LB film (Bushan et al., 1995).

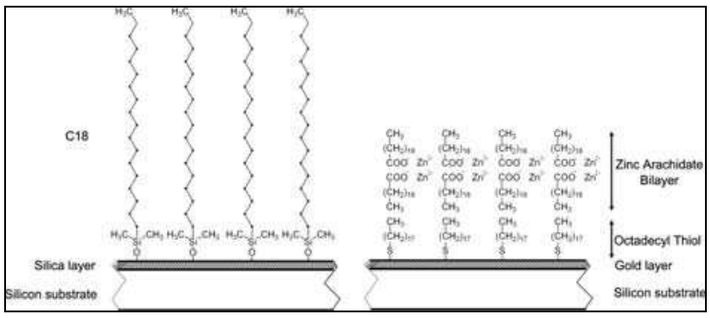

Fig. 7. The structures of C18 SAMs and zinc arachidate LB film. Both of the films possess long alkyl chains of C18. Reproduced from Bushan et al., 1995.

It is generally believed that strong affinity of the molecules to the substrate is a basic requirement for effective boundary lubrication. For SAMs with similar composition and structures, the stronger adhesion is, the better wear-resistance is expected to be achieved. For example, the chemisorption of alkylsilane/alkylthiol on the Si/Au substrate surface is realized by Si-O/Au-S covalent bonding, respectively. The bond energy of Au-S is lower than that of Si-O (Bushan et al., 2005). Thus, alkylsilane SAMs can withstand higher normal loads than the alkylthiol ones with the same alkyl chain and tail group (Bushan et al., 2005; Booth et al., 2009). Moreover, the cross-link of head groups may also play an important role in stabilizing the SAMs. For instance, owing to the intermolecularly cross-link of Si-O-Si between adjacent molecules, n-octadecyltrichlorosilane SAMs (OTS-SAMs, Fig. 8) possess much better wear resistance than n-octadecyldimethylchlorosilane SAMs (ODS-SAMs, Fig. 8) (Booth et al., 2009). However, comparing with alkylthiols, the cross-link of head groups causes chain distortion and the lack of long range order in the silane SAMs, both of which can serve as the energy-dissipating modes to increase the friction (Lio et al., 1997).

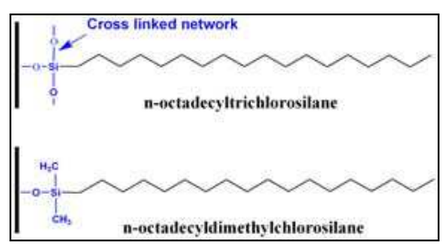

Fig. 8. Schematic structures of OTS-SAMs and ODS-SAMs.

The influence of alkyl chains

It has been proved that the frictional behaviors varied significantly with the alkyl chain length. SAMs with shorter chain length possesses higher friction coefficient (Xiao et al, 1996; McDermott et al., 1997) and lower load affording capability (Xiao et al, 1996; Bushan et al., 2005). To discover the origin of the chain length dependence, lots of works have been done. It is found that the frictional force is proportional to the contact area and shear strength (Tsukruk et al., 2001; b, Wang et al., 2005). Due to the loosely packed and disordered structures of the SAMs with shorter alkyl chain, on one hand, the contact area increases. On the other hand, CH_2-CH_2 backbones in a loosely packed SAMs are exposed to the AFM tip, which increases the van der Waals interaction between the tip and surface and thereby enhances the shear strength. So, it can be concluded that the microstructures, i.e., lower packing density and substantial disorder in SAMs, are key factors for the higher friction. In other words, the shorter chains are apt to form SAMs with more disorders which facilitate the energy-dissipation and give rise to a high friction and friction coefficient. The lower load affording capacity for the shorter chain SAMs is because that the shorter chains are less flexible to tile in response to the applied load (Chandross et al., 2005).

As the chain length increases to a critical value, the inter-chain attraction is large enough to form ordered structures and the chain length dependence is not so distinct. However, as discovered by Liu et al, the ultra-high compact density caused by the very long alkyl chain could result in a higher friction (Liu et al., 1996). For example, monolayers of dieicosyldimethylammonium bromide (Fig. 9, n=20, 22) are believed in a frozen state owing to the strong interchain interaction, while it is in a melted state for the molecules with short chain of C14. It is acordingly found that the monolayers of C14 yield a lower friction due to the compliant of the melted chains.

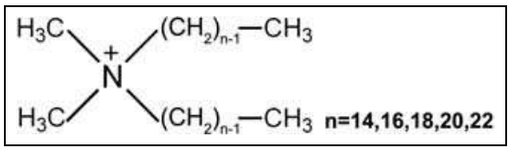

Fig. 9. The molecules investigated in the reference of Liu et al., 1996.

According to above interpretation, it seems that the chain length only has an indirect influence to affect the tribological performances by defects. To understand the direct correlation more clearly, lots of theoretical simulations have been performed (Chandross et al., 2005). It is observed that, for SAMs with no defects, longer chain length can endure heavier applied load. This is because that the longer chains are more flexible to tile in response to the applied load as compared to shorter ones. Moreover, for well-ordered, fully packed SAMs with different chain length of C6, C8 and C12, friction coefficient decreases as the chain carbon number increasing (Chandross et al., 2005). This is because that the effectiveness of stress transmission during sliding is dependent on the chain length–longer chains have more contact with neighboring ones. From the above discussions, it can be summarized that the frictional behaviors are influenced by the chains length due to the formed defects or the intrinsic difference between short and long alkyl chains.

The influence of tail groups

The tail groups exposed to the ambient environment have a significant effect on the surface nature of SAMs, such as wettability and adhesion (Tsukruk et al., 2001). Generally, the adhesion force (F_{ad}) between surfaces includes the capillary force (F_C), van der Waals forces

(F_{vdW}), electrostatic force (F_E), and chemical bonding force (F_B), which is described by equation (5):

$$F_{ad} = F_C + F_{vdW} + F_E + F_B \tag{5}$$

In ambient air conditions, F_C is proportional to the cosine value of water contact angle ($cos\theta$) on the surface and takes main contribution to the adhesion. Generally, lower surface energy corresponds to a hydrophobic surface, which has a high water contact angle (lower $cos\theta$ value) and thereby result in a lower F_C and then a lower F_{ad}. In liquid medium, F_C is eliminated and the adhesive force between different tail groups can be measured by CFM. It is observed that the adhesive forces between –COOH and –CH_3 groups are reduced in the following order: COOH/COOH >CH_3/CH_3 >COOH/CH_3 (Fig. 10a) (Noy et al., 1995). The adhesive force difference between COOH/COOH and CH_3/CH_3 may be result from the item of F_B. Specifically, the COOH polar groups tend to form intermolecolar hydrogen bonding to boost the chemical bonding force. Compared with the asymmetric pair of COOH/CH_3, the adhesive force for CH_3/CH_3 is higher. This can be explained as follows: the adhesive force is the product of tip radius R and adhesive work W_{st}, specifically,

$$F_{ad} = 1.5\pi R W_{st}, (W_{st} = \gamma_s + \gamma_t - \gamma_{st}) \tag{6}$$

where γ_s, γ_t and γ_{st} are the surface energy of sample, CFM tip and interface energy between them, respectively (Noy et al., 1995; Tsukruk et al., 1998). For the symmetric pair of CH_3/CH_3, the null interface energy γ_{st} will result in a higher adhesive work and adhesive force. Correspondingly, friction of different pairs are arranged in the same order, viz, COOH/COOH >CH_3/CH_3 >COOH/CH_3 (Fig. 10b)

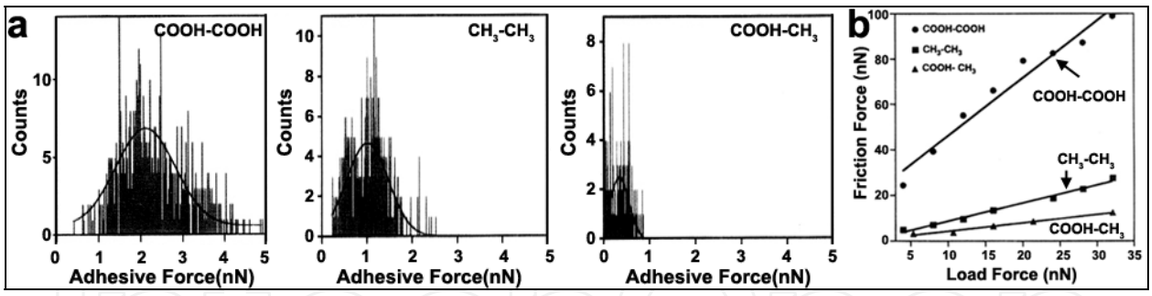

Fig. 10. Adhesion and friction for different pairs. Reproduced from Noy et al., 1995.

F_E is always generated between the charged tip and the charged samples. When tested in liquid medium, F_E is dependent on not only the nature of tail groups but also the pH value of the aqueous solution (Tsukruk & Blivnyuk, 1998). To be specific, in the pH range of pK_1~pK_2 (pK_1 and pK_2 are the isoelectric points of the sample and the tip, respectively, Fig. 11), attraction between the tip and sample is generated, which result in a high friction. In the cases of pH value lower than pK_1 or higher than pK_2, repulsion and lower friction is correspondingly obtained.

The spatial orientation of the tail groups also has a prominent impact on adhesion and friction. For example, an "odd-even" effect is observed for SAMs with same tail groups but different CH_2 number (odd or even) in the alkyl chain (Chang et al., 1994; Lee et al., 2001; Smith & Porter, 1993; Tao, 1993; Wong et al., 1998). As shown in Fig. 12, the spatial orientation of the –COOH tail groups are different for the two SAMs with odd or even

number of CH_2 units. As a result, intra-film hydrogen bonds are produced within a film for the pairs of odd-COOH SAMs, while inter-film hydrogen bonds are gegerated between the two surfaces for the pairs of even-COOH SAMs. It is then expectedly found that higher adhesion and friction were obtained for the pairs of even-COOH surfaces due to the inter-film hydrogen bonds. (Kim & Houston, 2000).

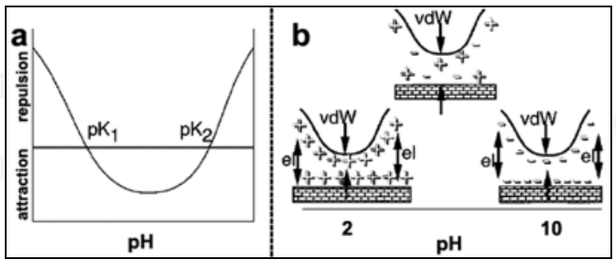

Fig. 11. Expected variation of adhesion-repulsion balance for interacting surfaces with two isoelectric points (a), and a scheme of tip/surface pairs with different surface charge distributions and force balances at different pH values (b). Reproduced from Tsukruk & Blivnyuk, 1998.

Based on the surface energy, tail groups of SAMs can be sorted into two categories of polar terminal groups (such as -OH, $-NH_2$, and -COOH) with high surface energy and apolar terminal groups (such as $-CH_3$ and $-CF_3$) with low surface energy. The SAMs with apolar terminal groups generally possess lower surface energy and relatively weak interaction between two sliding surfaces, which result in a lower adhesion and less energy loss leading to a lower friction force (Liu et al., 1996; Tsukruk et al., 1996; Zhang et al., 2002). However, although the surface energy of $-CF_3$ (12.9 mJ/m^2) is lower than that of $-CH_3$ (~24 mJ/m^2) (Bushan et al., 2005; Luengo et al., 1997), the fluorocarbon SAMs produce higher friction in AFM studies (Bushan et al., 2005; Kim et al., 1997; Peach et al., 1996; Houston et al., 2005). The unexpected higher friction is attributed to the larger size and higher electronegativity of the fluorine atom, which result in two major variations in the surface properties of SAMs (Kim et al., 1997). On one hand, the replacement of $-CH_3$ with larger tail groups of $-CF_3$ into the close-packed $\left(\sqrt{3}\times\sqrt{3}\right)$ R30^o lattice gives rise to increased surface steric interactions.

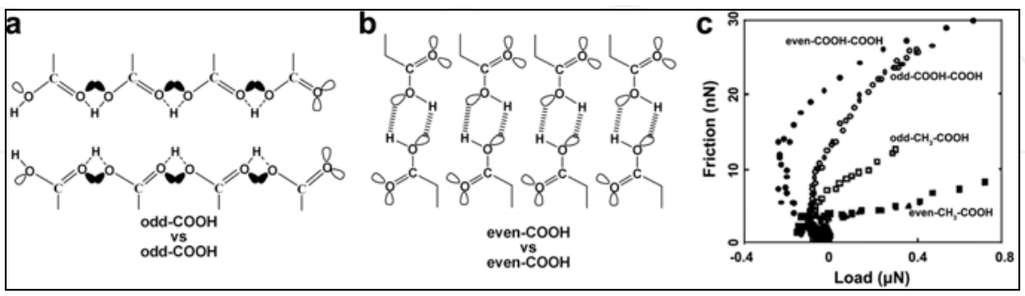

Fig. 12. A schematic representation of the -COOH end group orientations for alkanethiol SAMs having both odd and even numbers of methylene groups (a) and the plots of the lateral friction force vs. interfacial force for various end-group combinations (b). Reproduced from Kim & Houston, 2000.

During sliding, more energy is imparted to the film to overcome the consequent increased steric barriers and then results in higher friction (Kim et al., 1997; Peach et al, 1996). On the

other hand, the strong surface dipoles in CF_3-teminated monolayer would cause much higher attractive force between the AFM tip and the surface of SAMs, and eventually cause more energy loss to increase the friction (Houston, 2005). This size effect is also observed between the tail groups of $-CH(CH_3)_2$ and $-CH_3$ (Kim et al., 1999) as well as C60, phenyl and $-CH_3$ (Lee et al., 2001).

2.2 Mixed SAMs

Co-deposition of molecules with different terminal groups or alkyl chain lengths to form mixed SAMs is also extensively studied, which allows an in-depth understanding of the relationship between structure and performance of SAMs. Several reports have revealed the frictional behaviors of the mixed SAMs derived from akanethiols or alkylsilanes. For instance, the mixed monolayers with chemically heterogeneous surface composed of mercaptoundecanoic acid (MUA) and dodecanethiol (DDT) or mercaptoundecanol (MUO) and DDT have been prepared (Brewer & Leggett, 2004; Beake & Leggett, 1999). SFM tips immoblized with COOH or CH_3 groups were applied as the probes to investigate the tribological behaviors. As shown in Table 1, the adhesion for the symmetric pairs (polar-polar or apolar-apolar) is relatively higher, which can be well understood by referring to the equation (6), where γ_{st} is much lower for the symmetric pairs. The surface composition of the mixed SAMs can be reflected by the water contact angle θ. In other words, high fraction of polar group-terminated adsorbate (*e.g.* MUO) will produce a small θ and high $\cos\theta$ value. The relationship between friction coefficient and $\cos\theta$ is depicted in Fig. 13. It can be seen that, when COOH tip is applied, friction coefficient increases with increasing the $\cos\theta$ (i.e., increasing the MUO fraction). Correspondingly, when CH_3 tip is applied, friction coefficient increases with decreasing the $\cos\theta$ (i.e., increasing the DDT fraction). It is therefore concluded that the friction coefficient increases due to the enhanced interaction of the symmetric tip-sample pairs.

Sample	Tip	
	COOH	CH_3
CH_3	0.57±0.17; 0.58±0.26	1.2±0.54
COOH	1.6±0.41; 2.1±0.85	0.78±0.26
OH	1.9±0.34	0.76±0.20

Table 1. Mean adhesion forces (nN) in ethanol between different tip-sample pairs. Obtained from Beake & Leggett, 1999.

When a non-modified Si_3N_4 tip was applied to investigate the tribological behaviors of MUA/DDT mixed SAMs, friction force increased with increasing the relative amounts of MUA in the mixed SAMs (Fig. 13c). This attributes to that higher MUA fraction raises the interaction between the scanning tip and the mixed SAMs, eventually increasing the energy dissipation and friction.

Studies on comparing the tribological properties of one-component SAMs with mixed ones are also performed. As revealed by Whitesides *et al.*, mixed SAMs composed of octadecanethiol (ODT) and dodecanethiol (DDT) on Au substrate exhibit higher friction than one-component SAMs (Fig. 14a) (Bain & Whiteside, 1989). Such difference is attributed to the different structures of the two SAMs. I.e. the one-component SAMs is well-ordered,

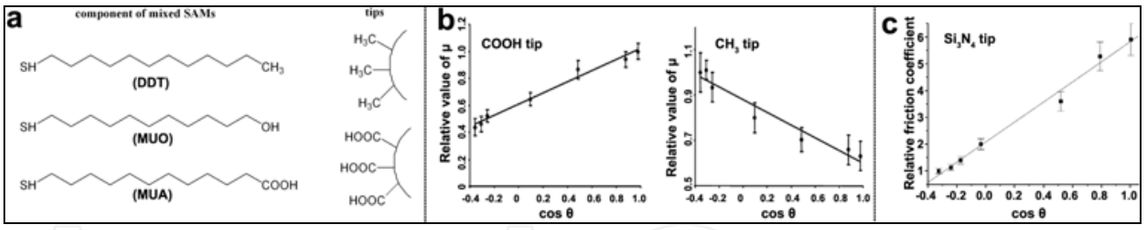

Fig. 13. The molecular structures of ODT, MUO, and MUA and the functionlized tips used to determine the tribological properties of the mixed SAMs (a); Friction coefficient as a function of cosθ for carboxylic acid-terminated tips and methyl-terminated tips (b); Correlation of relative friction coefficient with cosine of the water contact angle for mixed MUA/DDT monolayers (c). Reproduced from Brewer & Leggett, 2004 (b) and Beake & Leggett, 2000 (c).

while the mixed SAMs possess an outer region with disordered structure (Fig. 14b), which would increase the tip-sample interaction greatly and therefore producing a higher friction. However, a different tribological phenomenon has been observed for the mixed SAMs of alkylsilanes with different chain lengths on Si wafer. The friction for the mixed SAMs is lower than that of one-component SAMs. It is explained that the better lubrication performance of the mixed SAMs is attributed to the higher mobility of the tethered molecules in the monolayers, which can be evidenced by the much shorter relaxation time than that of one component SAMs (Zhang & Archer, 2003; Zhang & Archer, 2005).

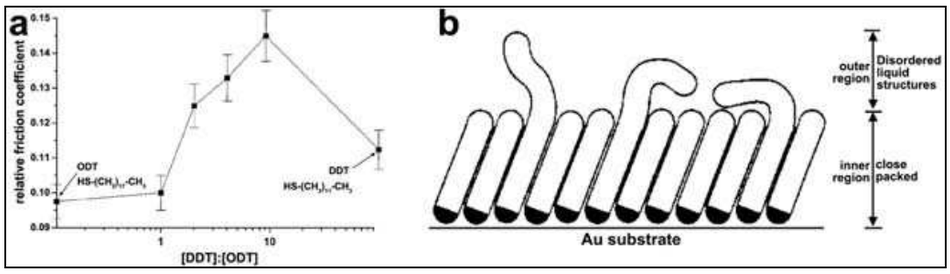

Fig. 14. Variation in relative friction coefficient with composition of mixed DDT/ODT monolayers (a); Structures of the mixed monolayers (b). Reproduced from Beake & Leggett, 2000 (a) and Bain & Whiteside, 1989 (b).

3. SAMFs

3.1 Functional group embedded SAMFs

As a potential lubricant in MEMS/NEMS, SAMs can reduce the adhesion and friction greatly. However, the load-carrying capacity of SAMs is relatively low, which significantly limits its service life. A promising way to further ameliorate the tribological behaviors of SAMs, especially the load-carrying capacity, is to enhance the stability of the films. It is revealed that the SAMFs with synergetic components generally exhibits longer anti-wear life (Ren et al., 2003; Ren et al., 2004; a, Song et al., 2008). The reason for the enhanced wear resistance is ascribed to the special structures of the SAMFs. Generally speaking, there are two approaches to construct SAMFs with unique structures, viz, one-step assembling and multi-step assembling. As to the one-step process, the pre-designed target precursors are assembled onto the substrate (Tam-Chang et al., 1995; Clegg & Hutchison, 1999; Clegg et al.,

1999; Song et al., 2006; Chambers et al., 2005); The multistep method involves common self-assembling and subsequent interface chemical reaction (Ren et al, 2003; Jiao et al., 2006). In most cases, the synthesis and the succedent purification for precursor molecules are too difficult to perform. So, compared to the one-step method, the stepwise strategy is more suitable to construct SAMFs with unique molecular architectures.

For SAMFs, the attachment to the substrate and the tail groups exposed to the ambient environment remain almost the same with SAMs. The most dramatic difference is related to the bulk chain. Specifically, the attraction between adjacent alkyl chains of normal SAMs is the weak van der Waals force. Within SAMFs, the inter-chain interaction is enhanced by functional groups, such as diacetylene (Mowery et al., 1999), peptide (Clegg & Hutchison, 1996; Sabapathy et al., 1998), and sulfone (Evans et al., 1991). It is hypothesized that the functional groups interact laterally taking the form of hydrogen bonding, dipole interaction, π-stacking, or covalent attachment, which are able to influence the integrity, stability and the tribological performances of the film (Ren et al., 2003; a, Song et al, 2008).

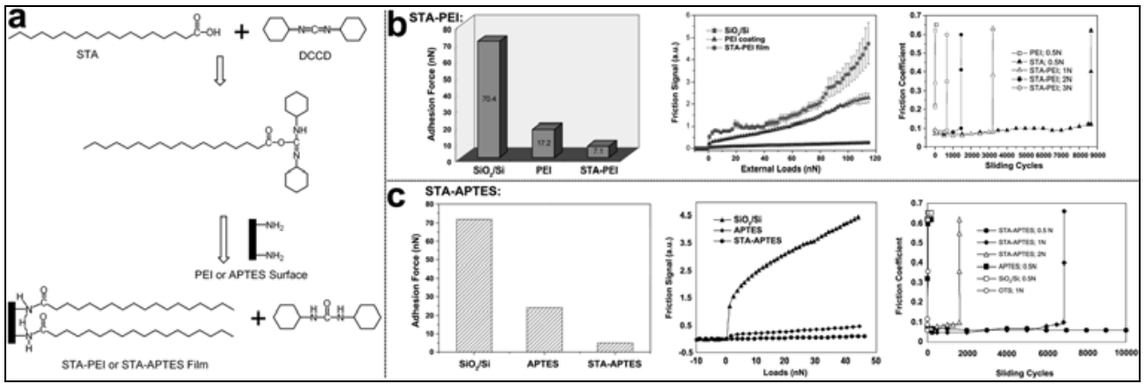

Fig. 15. Generation of an STA monolayer on PEI or APTES coated Si surface by chemical adsorption in the presence of N,N′-dicyclohexylcarbodiimide (DCCD) as a dehydrating agent in the reacting solution (a); Tribological behaviors of STA-PEI (b) and STA-APTES (c). Reproduced from Ren et al., 2004 (a, b), and Ren et al., 2003 (c).

To obtain nano film with promising application in the lubricant system of MEMS/NEMS, much effort in our group has been paid to construct a series of SAMFs with improved tribological properties better than SAMs. For example, taking advantage of amidation reaction between carboxyl (-COOH) and amine ($-NH_2$) groups, SAMFs consisting of 3-aminopropyl triethoxysilane (APTES) (Ren et al., 2003) or polyetherimide (PEI) (Ren et al., 2004) underlayer and stearic acid (STA) outerlayer has been prepared (Fig. 15a). The as-obtained SAMFs of STA-APTES and STA-PEI strongly attach to the substrate and possess a hydrophobic surface and a flexible alkyl chain outerlayers, which make them exhibiting excellent adhesion resistance and low nano-friction (Fig. 15b, c). Moreover, the interaction between adjacent chains intensified by the hydrogen bonding is assumed to be responsible for the improved wear resistance. Comparing with OTS-SAMs, the STA-APTES and STA-PEI SAMFs show much better load carrying and anti-wear capacity, demonstrating that the tribological properties of self-assembled films can be greatly improved by controlling the chemical structure and composition of the SAMFs.

To investigate the influence of underlayer structures on tribological properties, a systematical research has also been done in our group (b, Song et al., 2008). It is found that

the structures of underlayer have a great effect on the frictional behaviors. Specifically, SAMFs with different underlayers of APTES, N-[3-(trimethoxylsilyl)propyl]ethylenediamine (DA) or N-[3-(trimethoxylsilyl)propyl]-diethylenetriamine (TA) and indentical outerlayer of lauroyl chloride (coded as C12) have been constructed via amidation reaction (Fig. 16). As attenuated total reflection-Fourier transform infrared spectrometry (ATR-FTIR) analyses

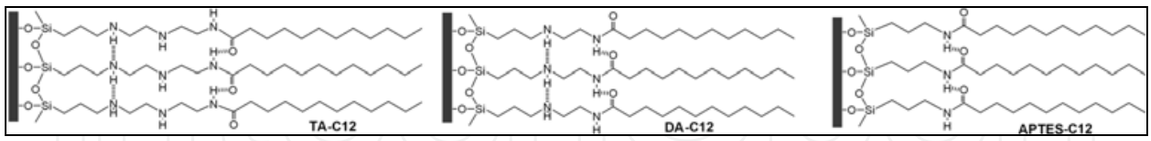

Fig. 16. Schematic structures of TA-C12, DA-C12, and APTES-C12 SAMFs.

indicated, the packing density of the as-prepared films follows the order DA-C12> TA-C12 > APTES-C12. The higher packing density of DA/TA-C12 is due to their longer chains of the underlayers. Even though TA has a longer molecular chain, TA-C12 is slightly less ordered than DA-C12, which is probably due to one more $-CH_2CH_2NH-$ unit contained in the chain of TA (one more $-CH_2CH_2NH-$ means that more random intermolecular hydrogen bonds could be formed between TA molecules). The lower packing density of APTES-C12 results in higher friction coefficient, both in nanoscale and macroscale.

In the above cases, the lateral interaction between adjacent chains is the weak hydrogen bonding. Zhao et al have constructed a triple-layer film (abridged as GAO) with lateral covalent network structures, which is composed of OTS outerlayer, APTES interlayer and 3-glycidoxypropyl-trimethoxysilane (GPTMS) underlayer (Zhao et al, 2009). The structure of the triple-layer film is depicted in Fig. 17a. It is belived that the APTES molecule serves as the linkage to combine the GPTMS with OTS. Specifically, the amine groups of APTES can react with the tail groups of GPTMS-SAMs and the hydroxyl groups formed by the hydroxylation are served as the active points to induce the self assembling of OTS molecules. The as-constructed film shows much better wear resistance as compared with OTS-SAMs, which is ascribed to the lateral Si-O-Si network structures (Fig. 17b).

3.2 Polymer SAMFs

The polymer nano-film with cross-linking network structures can sustain high compression and shear stress (Tsukruk et al., 1999; Luzinov et al., 2000; Luzinov et al., 2001; Maeda et al., 2002). So, polymeric thin film has been used as boundary lubricant coating in many fields including MEMS/NEMS, artificial joints, and computer hard disks, etc. However, physically adsorbed polymer films are easily peeled off during friction. Recently, there are two ways to construct chemically tethered polymer SAMFs, viz, "grafting to" or "grafting from" approaches. In a "grafting to" approach, the presynthesized end-functionalized polymer molecules react with a certain substrate to form polymer brushes. For example, a copolymer of poly[styrene-b-(ethylene-co-butylene)-b-styrene] (coded as SEBS) functionalized with 2% maleic anhydride into the hydrocarbon chains was assembled onto the surface of epoxy-terminated monolayer (Fig. 18a-d) (Luzinov et al., 2001). The as-fabricated films possess low friction coefficient, modest adhesion, low stiction, and good wear stability. To further improve the wear resistance, a SAMF with trilayer sandwiched architecture have been constructed (Fig. 18e, f) (Sidorenko et al., 2002). As expected, the anti wear life is much longer than epoxy composite layer (Fig. 18f).

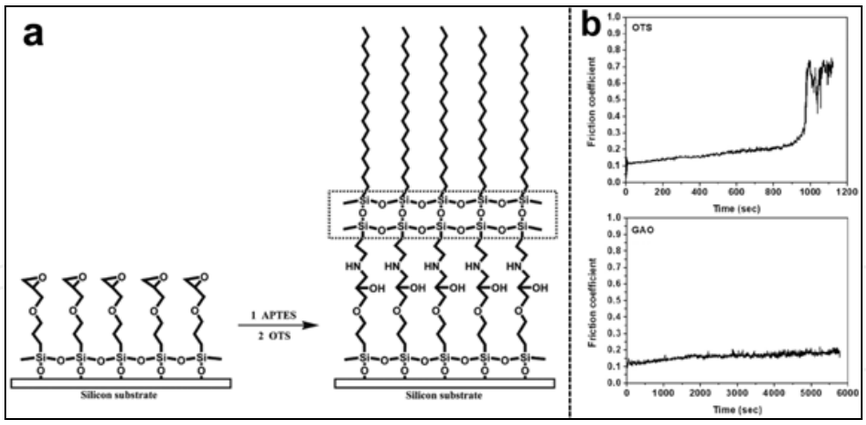

Fig. 17. Schematic structure and the strategy employed to prepare GAO triple-layer film (a); Variation in friction coefficient with time for OTS monolayer and GAO triple-layer film (b). Reproduced from Zhao et al., 2009.

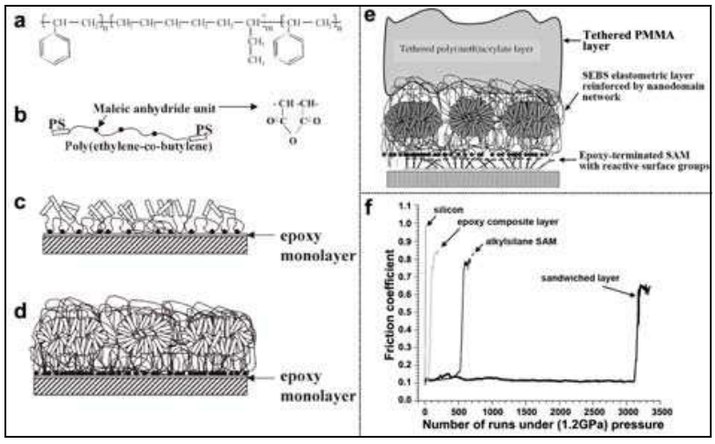

Fig. 18. Chemical (a) and schematic (b) structure of SEBE; SEBS layer with disordered structures and a thickness<2.5 nm (c); SEBS layer with nanodomain morphology and a thickness>2.5 nm (d); Architecture of sandwiched trilayer (e); Friction coefficient versus the number of reciprocal sliding runs for different samples (f). Reproduced from Luzinov et al., 2001 (a-d) and Sidorenko et al., 2002 (e, f).

However, few species of polymers can be immobilized onto the surface by "grafting to" approach due to the following two considerations (Zhao & Brittain, 2000). On one hand, it is difficult to synthesis polymer with functional anchoring groups. On the other hand, the as-synthesized polymer has complicated chain structures, which result in a low grafting density and thick film thickness. To circumvent this problem, "grafting from" approach has been proposed to prepare relatively thicker polymer brush with a higher grafting density. A representative "grafting from" approach, also called surface initiated polymerization (SIP), includes steps of introducing initiators on the substrate surface and succedent in-situ polymerization. Generally speaking, the immobilization of initiators is achieved by forming initiator-containing SAMs on the substrate. For instance, Takahara et al has prepared covalently tethered poly(methyl methacrylate) (PMMA) brushes on the Si wafer immobilized with an initiator SAMs of 2-bromoisobutylate moiety, abridged as DMSB (Fig.

19a) (Sakata et al., 2005). Compared with the spin-coated PMMA film, the self-assembled PMMA brush is found possessing much better wear resistance (Fig. 19b). However, this kind of initiator with complex molecular structure is also difficult to synthesis. Zhou et al. has developed a novel and much easier strategy to prepare PMMA film with comparable thickness based on the surface radical chain-transfer reaction (Zhou et al., 2001). The basic strategy of this novel process is depicted in Fig. 19c. It is clearly shown that, during this simple SIP process, the Si substrate was pre-modified by a SAMs of mercaptopropyltrimethoxylsilane (MPTES) rather than the complex initiators. As revealed by Yan et al, polystyrene (PSt) film can also be prepared by the same procedure (Zhao et al., 2008). The covalently tethered PSt film showed excellent scratch and adhesion resistance (Fig. 19d).

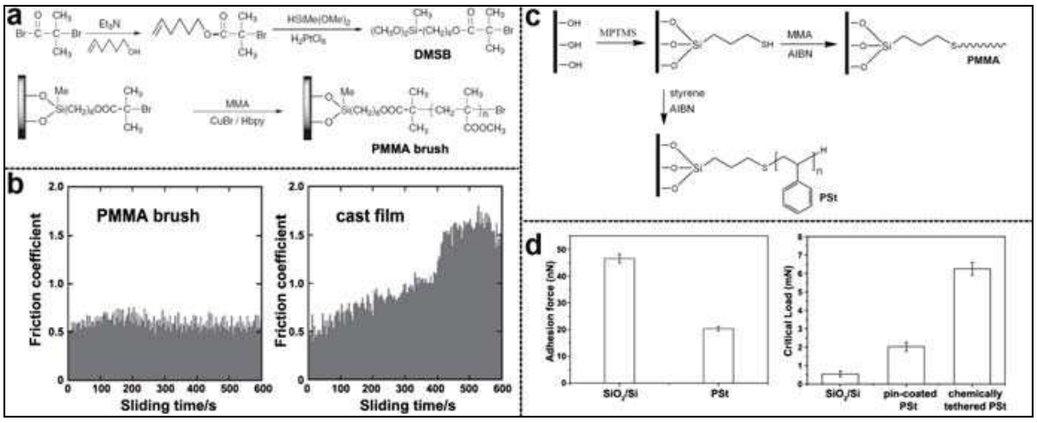

Fig. 19. The synthesis of DMSB and the PMMA brush (a); Friction coefficient versus sliding time for PMMA brush and cast film under a load of 0.49 N at a sliding velocity of 90 mm/min in air (b); A simple strategy to prepare PMMA and PSt brush (c); (d) Adhesion and scratch resistance of the PSt brush. Reproduced from Sakata et al., 2005 (a, b), Zhou et al., 2001 (c) and Zhao et al., 2008 (c, d).

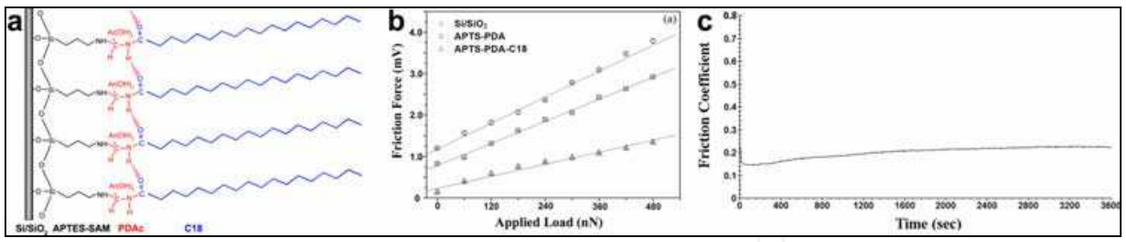

Fig. 20. A schematic view for the formation and combination bonding of the 3-layer film on silicon wafer (a); The nano- and macrotribological behaviors of different samples (b). Reproduced from Ou et al., 2009.

Recently, inspired by the "structure-property" correlation of SAMs, a robust polymer-based film has been constructed in our group by adopting APTES-SAMs as "headgroup", polydopamine (PDA) as "bulk chain", and stearoyl chloride SAMs as "tailgroup" (Ou et al., 2009). The in-situ polymerization of PDA on the APTES-SAMs surface is more like "grafting from" approach. The inherent special chemical structure, viz, the high adhesion to the substrate, the covalent combination between adjacent layers, the cross-linked PDA, as well

as the hydrophobic and flexible C18 chain, takes main responsibility for the enhanced load-carrying capacity and lengthened anti-wear life (Fig. 20).

4. SAIFs and SAO-ICFs

Zirconia (ZrO_2) and ZrO_2 based nanocomposite film is a popular candidate for lubricant coating in nano-devices. Several different methods, such as physical vapor deposition and plasma spraying, have been established to prepare ZrO_2 based nanocomposite film (Pakala et al., 1997). High quality films with uniform structure, good compactness and high adherence to the substrate can be obtained by these techniques. However, some strategies need large apparatus and are high energy-consuming. Therefore, lots of efforts have been made to develop novel and feasible technique for deposition of ZrO_2 nanofilm and ZrO_2 based nanocomposite film. Among these researches, aqueous deposition onto SAMs with particular functional tail groups, such as $–SO_3H$ (Wang et al., 2004; Wang et al., 2005; Zlotnikov et al., 2008), $–PO(OH)_2$ (Zhang et al., 2006) and –OH (Ou et al., 2001), are studied intensively. For example, Wang et al. have prepared a crystalline ZrO_2-SAIFs on the Si substrate mediated by a sulfonated MPTES-SAMs (Fig. 21a) (Wang et al., 2004; Wang et al., 2005). As experimental results shown, the as-deposited ZrO_2-SAIFs is characterized by poor mechanical and tribological behaviors (Fig. 21b), which may be ascribed to the loose-packed structures caused by defects. Fortunately, it is found that a simple post-annealing (Fig. 21b) (Wang et al., 2005) or a unique preparation process with high pressure (Fig. 21c, d) (Zhang et al., 2006) can ameliorate the mechanical and tribological properties effectively.

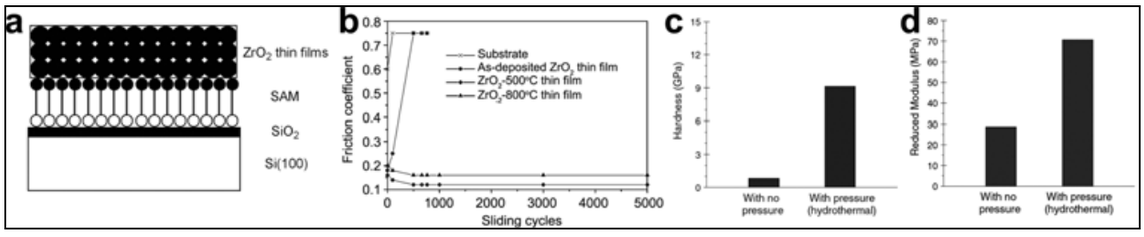

Fig. 21. Schematic of growth of ZrO_2 thin film on SAMs in aqueous medium (a); Friction coefficients as a function of sliding cycles at a load of 0.5 N (b); Mechanical properties of the ZrO_2 films prepared with a hydrothermal process at 135 ^oC, ~5 atm, for 24 h, as compared to those prepared with no pressure (c, d). Reproduced from Wang et al., 2004 (a), Wang et al., 2005 (b) and Zhang et al., 2006 (c, d).

To prepare ZrO_2 based SAO-ICFs, layer-by-layer (LbL) assembly technique is often applied. Generally speaking, LbL technique is based on sequential adsorption of oppositely charged materials, such as polyelectrolytes and inorganic nanomaterials. For example, Claus *et al* have obtained a superhard ZrO_2/PSS SAO-ICFs by a LbL process which is based on the electrostatic interaction between ZrO_2 nanoparticles (positive charged) and PSS (negative charged) (Fig. 22) (Rosidian et al., 1998).

However, this electrostatic LbL technique is confined to the charged materials. To expand the appliction of the LbL, a novel non-electrostatic layer-by-layer (NELbL) assembly technique has been invented in our group (Ou et al., 2010). The newly-reported PDA is served as the building block for its special nature, viz, high adhesion to almost all surfaces and the active surface with functional groups (such as –OH and $–NH_2$). As schematically illustrated in Fig. 23, PDA can be chemically grafted onto the amine groups of APTES-SAMs

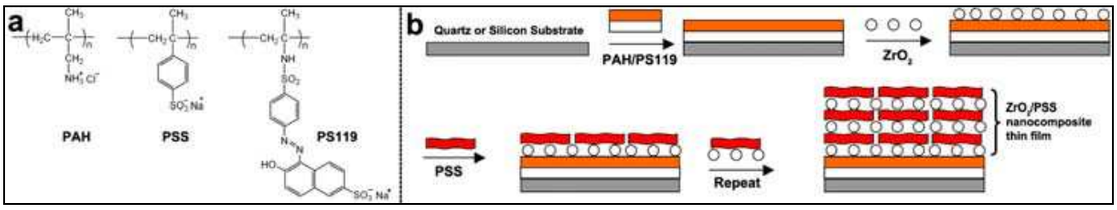

Fig. 22. The molecular structures of PAH, PSS and PS119 (a); Schematic of multilayer fabrication of ZrO_2/PSS SAO-ICF (b). Reproduced from Rosidian et al., 1998.

(Fig. 23, Process II) or hydroxyl groups of ZrO_2 film (Fig. 23, Process IV). Besides, the ZrO_2 clusters formed in the $Zr(SO_4)_2$ solution can deposit onto the PDA surface via chelation (Fig. 23, Process III). Thus, the sequential deposition of ZrO_2 and PDA can present a novel non-electrostatic strategy to construct ZrO_2/PDA SAO-ICFs. The microhardness and elastic modulus of the annealed 15-cycle ZrO_2/PDA film are measured to be as high as 24.10 and 250 GPa, respectively. This microhardness is comparable with that of ZrO_2/PSS SAO-ICF (25.13 GPa) (Rosidian et al., 1998). The outstanding mechanical properties of the ZrO_2/PDA SAO-ICFs can be ascribed to the in-suit deposition and organic-inorganic hybrid microstructures (Ou et al., 2001).

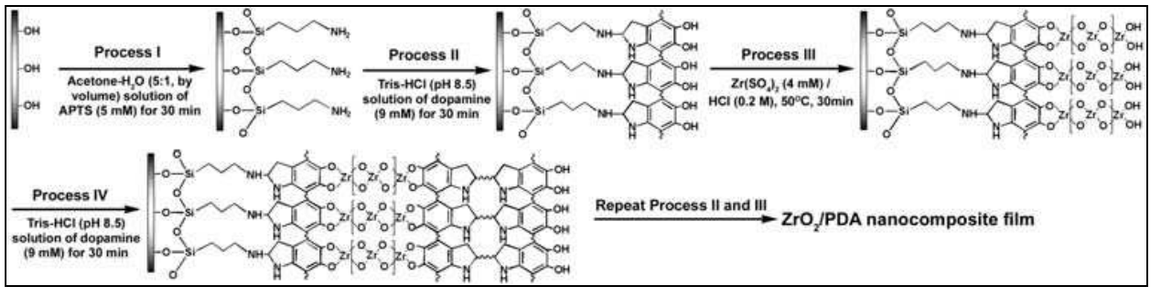

Fig. 23. A schematic view for constructing ZrO_2/PDA SAO-ICFs. Reproduced from Ou et al., 2001.

5. Conclusion

Based on the above discussions, it can be obtained that the tribological behaviors of SANFs are mainly structure dependent. Namely, the interfacial and interfilm interaction is supposed to influence the tribological properties of the prepared SANFs. With the efforts of many researchers, principal dependence between tribological performance and different parts of SAMs, viz, head/tail groups and bulk chains, has been proposed. This can be a basic understanding for us to investigate more complicated systems, such as SAMFs, SAIFs and SAO-ICFs. It is expected that the extracted "structures-properties" correlation can serve as the guidance to direct the further designing of lubricant coatings for MEMS/NEMS and other devices in molecule-level.

6. References

Bain, C. & Whitesides, G. (1989) Formation of monolayers by the coadsorption of thiols on gold-variation in the length of the alkyl chain. *Journal of the American Chemical Society*, Vol. 111, No. 18, (Aug, 1989) 7164-7175, 0002-7863.

Bushan, B.; Kulkarni, A.; Koinkar, V.; Boehm, M.; Odoin, L.; Martelet, C. & Belin, M. (1995) Microtribological characterization of self-assembled and langmuir-blodgett monolayers by atomic and friction force microscopy. *Langmuir*, Vol. 11, No. 8 (Aug, 1995) 3189-3198, 0743-7463.

Bliznyuk, V.; Everson, M. & Tsukruk, V. (1998) Nanotribological properties of organic boundary lubricants: Langmuir films versus self-assembled monolayers. *Journal of Tribology-Transactions of the Asme,* Vol. 120, No. 3 (Jul, 1998) 489-495, 0742-4787.

Beake, B. & Leggett, G. (1999) Friction and adhesion of mixed self-assembled monolayers studied by chemical force microscopy. *Physical Chemistry Chemical Physics,* Vol. 1, No. 14, (Jul, 1999) 3345-3350, 1463-9076.

Beake, B. & Leggett, G. (2000) Variation of frictional forces in air with the compositions of heterogeneous organic surfaces. *Langmuir* Vol. 16, No. 2, (Jan, 2000) 735-739, 0743-7463.

Brewer, N.; Beaker, B.; Leggett, G. (2001) Friction force microscopy of self-assembled monolayers: Influence of adsorbate alkyl chain length, terminal group chemistry, and scan velocity. *Langmuir,* Vol. 17, No. 6, (Mar, 2001) 1970-1974, 0743-7463.

Brewer, N. & Leggett, G. (2004) Chemical force microscopy of mixed self-assembled monolayers of alkanethiols on gold: Evidence for phase separation. *Langmuir*, Vol. 20, No. 10, (May, 2004) 4109-4115, 0743-7463.

Butt, H.; Cappella, B.; & Kappl, M. (2005) Force measurements with the atomic force microscope: technique, interpretation and applications. *Surface Science Reports,* Vol. 59, (Aug, 2005) 1-152, 0167-5729.

Bushan, B.; Kasai, T.; Kulik, G.; Barbieri, L. & Hoffmann, P. (2005) AFM study of perfluoroalkylsilane and alkylsilane self-assembled monolayers for anti-stiction in MEMS/NEMS. *Ultramicroscopy,* Vol. 105, No, 1-4 (Nov, 2005) 176-188, 0304-3991.

Booth, B.; Vilt, S.; McCabe, C. & Jennings, G. (2009) Tribology of Monolayer Films: Comparison between n-Alkanethiols on Gold and n-Alkyl Trichlorosilanes on Silicon. *Langmuir*, Vol. 25, No. 17 (Sep, 2009) 9995-10001, 0743-7463.

Chang, S.; Chao, L. & Tao, Y. (1994) Structures of self-assembled monolayers of aromatic-derivatized thiols on evaporated gold and silver surfaces-implication on packing mechanism. *Journal of the American Chemical Society.* Vol. 116, No. 15, (Jul, 1994) 6792-6805, 0002-7863.

Clegg, R. S. & Hutchison, J. E. (1996) Hydrogen-bonding, self-assembled monolayers: Ordered molecular films for study of through-peptide electron transfer. *Langmuir,* Vol. 12, No. 22, (Oct,1996) 5239-5243, 0743-7463

Clegg, R. & Hutchison, J. (1999) Control of monolayer assembly structure by hydrogen bonding rather than by adsorbate-substrate templating. *Journal of the American Chemical Society*, Vol. 121, No. 22, (Jun, 1999) 5319-5327, 0002-7863.

Clegg, R.; Reed, S.; Smith, R.; Barron, B.; Rear, J. & Hutchison, J. (1999) The interplay of lateral and tiered interactions in stratified self-organized molecular assemblies. *Langmuir,* Vol. 15, No. 26, (Dec, 1999) 8876-8883, 0743-7463.

Cappella, B. & Dietler, G. (1999) Force-distance curves by atomic force microscopy. *Surface Science Reports,* Vol. 34, No. 1, (July, 1999) 1-104, 0167-5729.

Chambers, R.; Inman, C. & Hutchison, J. (2005) Electrochemical detection of nanoscale phase separation in binary self-assembled monolayers. *Langmuir*, Vol. 21, No. 10, (May, 2005) 4615-4621, 0743-7463.

Chandross, M.; Lorenz, C.; Grest, G.; Stevens, M. & Webb III, E. (2005) Nanotribology of anti-friction coatings in MEMS. *Journal of the Minerals, Metals and Materials Society,* Vol. 57, No. 9, (Sep, 2005) 55-61, 1047-4838.

DePalma, V. & Tillman, N. (1989) Friction and wear of self-assembled trichlorosilane monolayer films on silicon. *Langmuir,* Vol. 5, No. 3, (May-Jun, 1989) 868-872, 0743-7463.

Evans, S.; Urankar, E.; Ulman, A. & Ferris, N. (1991) Self-assembled multilayers of omega-mercaptoalkanoic acids-selective ionic interactions. *Journal of the American Chemical Society*, Vol. 113, No. 15, (Jul, 1991) 5866-5868, 0002-7863.

Foisner, J.; Glaser, A.; Leitner, T.; Hoffmann, H. & Friedbacher, G. (2004) Effects of surface hydrophobization on the growth of self-assembled monolayers on silicon. *Langmuir,* Vol. 20, No. 7, (Mar, 2004), 2701-2706, 0743-7463.

Foster, T.; Alexander, M.; Leggett, G.; McAlpine, E. (2006) Friction force microscopy of alkylphosphonic acid and carboxylic acids adsorbed on the native oxide of aluminum. *Langmuir,* Vol. 22, No. 22, (Oct, 2006) 9254-9259, 0743-7463.

Gulino, A.; Mineo, P.; Scamporrino, E.; Vitalini, D. & Fragala, I. (2004) Molecularly engineered silica surfaces with an assembled porphyrin monolayer as optical NO_2 molecular recognizers. *Chemistry of Materials,* Vol. 16, No. 10, (May, 2004), 1838-1840: 0897-4756.

Houston, J. & Michalske, T. (1992) The interfacial-force microscope. *Nature,* Vol. 356, No. 6366, (March, 1992) 266-267, 0028-0836.

Houston, J.; Doelling, C.; Vanderlick, T.; Hu, Y.; Scoles, G.; Wenzl, I.; Lee, T. (2005) Comparative study of adhesion, friction, and mechanical properties of CF_3- and CH_3- terminated alkanethiol monolayers. *Langmuir,* Vol. 21, No. 9 (Apr, 2005) 3926-3932, 0743-7463.

Hsu, S. (2004) Nano-lubrication: concept and design. *Tribology International*, Vol. 37, No, 7, (Jul, 2004), 537-545, 0301-679X.

Jiao, J.; Anariba, F.; Tiznado, H.; Schmidt, I.; Lindsey, J.; Zaera, F. & Bocian, D. (2006) Stepwise formation and characterization of covalently linked multiporphyrin-imide architectures on Si(100). *Journal of the American Chemical Society*, Vol. 128, No. 21, (May, 2006) 6965-6974, 0002-7863.

Kim, H.; Koini, T.; Lee, R. & Perry S. (1997) Systematic studies of the frictional properties of fluorinated monolayers with atomic force microscopy: Comparison of CF_3- and CH_3-terminated films. *Langmuir* Vol. 13, No. 26, (Dec, 1997) 7192-7196, 0743-7463.

Kim, H.; Graupe, M.; Oloba, O.; Koini, T.; Imaduddin, S.; Lee, T. & Perry, S. (1999) Molecularly specific studies of the frictional properties of monolayer films: A systematic comparison of CF_3-, $(CH_3)_2CH$-, and CH_3-terminated films. *Langmuir*, Vol. 15, No. 9 (Apr, 1999) 3179-3185, 0743-7463.

Kim, H. & Houston, J. (2000) Separating mechanical and chemical contributions to molecular-level friction. *Journal of the American Chemical Society.* Vol. 122, No. 48, (Dec, 2000) 12045-12046, 0002-7863.

Liu, Y.; Evans, D.; Song, Q. & Grainger, D. (1996) Structure and frictional properties of self-assembled surfactant monolayers. *Langmuir,* Vol. 12, No. 5, (Mar, 1996), 1235-1244, 0743-7463.

Lio, A.; Charych, D. & Salmeron, M. (1997) Comparative atomic force microscopy study of the chain length dependence of frictional properties of alkanethiols on gold and

alkylsilanes on mica. *The Journal of Physical Chemistry B,* Vol. 101, No. 19, (May, 1997) 3800-3805, 1520-6106.

Luengo, G.; Campbell, S.; Srdanov, V.; Wudl, F. & Israelachvili, J. (1997) Measurement of the adhesion and friction of smooth C60 surfaces. *Chemistry of materials,* Vol. 9, No. 5, (May, 1997) 1166-1171, 0897-4756.

Li, J.; Wang, C.; Shang, G.; Xu, Q.; Lin, Z.; Guan, J.; Bai, C. (1999) Friction coefficients derived from apparent height variations in contact mode atomic force microscopy images. *Langmuir,* Vol. 15, No. 22, (Oct, 1999) 7662-7669, 0743-7463.

Lee, S.; Puck, A.; Graupe, M.; Colorada, R.; Shon, Y.; Lee, T. & Perry, S. (2001) Structure, wettability, and frictional properties of phenyl-terminated self-assembled monolayers on gold. *Langmuir,* Vol. 17, No. 23, (Nov, 2001) 7364-7370, 0743-7463.

Luzinov, I.; Julthongpiput, D.; Liebmann-Vinson, A.; Cregger, T.; Foster, M. & Tsukruk, V. (2000) Epoxy-terminated self-assembled monolayers: Molecular glues for polymer layers. *Langmuir* Vol., 16, No. 2, (Jan, 2000) 504-516, 0743-7463.

Luzinov, I.; Julthongpiput, D.; Gorbunov, V. & Tsukruk, V. (2001) Nanotribological behavior of tethered reinforced polymer nanolayer coatings. *Tribology International,* Vol. 34, No. 5, (May, 2001) 327-333, 0301-679X.

Leggett, G.; Brewer, N.; Chong, K. (2005) Friction force microscopy: towards quantitative analysis of molecular organisation with nanometre spatial resolution. *Physical Chemistry Chemical Physics,* Vol. 7, No. 6, (Feb, 2005) 1107-1120, 1463-9076.

Love, J.; Estroff, L.; Kriebel, J.; Nuzzo, R.; Whitesides, G. (2005) Self-assembled monolayers of thiolates on metals as a form of nanotechnology. *Chemical Reviews,* Vol. 105, No. 4 (Apr, 2005) 1103-1169.

McDermott, M.; Green, J. & Porter, M. (1997) Scanning force microscopic exploration of the lubrication capabilities of n-alkanethiolate monolayers chemisorbed at gold structural basis of microscopic friction and wear. *Langmuir,* Vol.13, No. 9, (Apr, 1997) 2504-2510, 0743-7463.

Mowery, M.; Kopta, S.; Ogletree, D.; Salmeron, M. & Evans C. (1999) Structural manipulation of the frictional properties of linear polymers in single molecular layers. *Langmuir,* Vol. 15, No. 15, (Jul, 1999) 5118-5122, 0743-7463.

Maeda, N.; Chen, N.; Tirrell, M. & Israelachvili, J. (2002) Adhesion and friction mechanisms of polymer-on-polymer surfaces. *Science,* Vol. 297, No.5580, (Jul, 2002) 379-382, 0036-8075.

Noy, A.; Frisbie, C.; Rozsnyai, L.; Wrighton, M. & Lieber, C. (1995) Chemical force microscopy-exploiting chemically-modified tips to quantify adhesion, friction, and functional-group distributions in molecular assemblies. *Journal of the American Chemical Society,* Vol. 117, No. 30, (Aug, 1995), 7943-7951, 0002-7863.

Noy, A.; Vezenov, D. & Lieber, C. (1997) Chemical force microscopy. *Annual Review of Materials Science,* Vol. 27, (Aug, 1997) 381-421, 0084-6600.

Ou, J.; Wang, J.; Liu, S.; Zhou, J.; Yang, S. (2009) Self-assembly and tribological property of a novel 3-layer organic film on silicon wafer with polydopamine coating as the interlayer. *The Journal of Physical Chemistry C,* Vol. 113, No, 47, (Nov, 2009) 20429-20434, 1932-7447.

Ou, J.; Wang, J.; Qiu, Y.; Liu, L. & Yang, S. (2010) Mechanical property and corrosion resistance of zirconia/polydopamine nanocomposite multilayer films fabricated via

a novel non-electrostatic layer-by-layer assembly technique. *Surface and Interface Analysis,* DOI: 10.1002/sia.3631, 1096-9918.

Ostuni, E.; Yan, L. & Whitesides, G. M. (1999) The interaction of proteins and cells with self-assembled monolayers of alkanethiolates on gold and silver. *Colloids and Surfaces B-Biointerfaces*, Vol 15, No. 1, (Aug, 1999), 3-30, 0927-7765.

Overney, R.; Meyer, E.; Frommer, J.; Brodbeck, D.; Lüthi, R.; Howald, L.; Güntherodt, H.; Fujihira, M.; Takano, H. & Gotoh, Y. (1992) Friction measurements on phase-separated thin-films with a modified atomic force microscope. *Nature,* Vol 359. No. 6391, (Sep, 1992), 133-135, 0028-0836.

Peach, S.; Polak, R. & Franck, C. (1996) Characterization of partial monolayers on glass using friction force microscopy. *Langmuir*, Vol. 12, No. 25 (Dec, 1996) 6053-6058, 0743-7463.

Pakala, M.; Walls, H. & Lin, R. (1997) Microhardness of sputter-deposited zirconia films on silicon wafers. Journal of the American Ceramic Society, Vol. 80, No. 6, (Jun, 1997) 1477-1484, 0002-7820.

Rosidian, A.; Liu, Y. & Claus, R. (1998) Ionic self-assembly of ultrahard ZrO_2/polymer nanocomposite thin films. *Advanced Materials,* Vol. 10, No. 14, (Oct, 1998) 1087-1091, 0935-9648.

Ren, S.; Yang, S. & Zhao, Y. (2003) Micro- and macro-tribological study on a self-assembled dual-layer film. *Langmuir,* Vol. 19, No. 7, (Apr, 2003), 2763-2767, 0743-7463.

Ren, S.; Yang, S.; Wang, J.; Liu, W. & Zhao, Y. (2004) Preparation and tribological studies of stearic acid self-assembled monolayers on polymer-coated silicon surface. *Chemistry of Materials,* Vol. 16, No. 3, (Feb, 2004) 428-433, 0897-4756.

Smith, E. & Porter, M. (1993) Structure of monolayers of short-chain n-alkanoic acids ($CH_3(CH_2)_nCOOH$, n = 0-9) spontaneously adsorbed from the gas-phase at silver as probed by infrared reflection spectroscopy. *The Journal of physical chemistry,* Vol. 97, No. 30, (Jul, 1993), 8032-8038, 0022-3654.

Sabapathy, R.; Bhattacharyya S.; Leavy, M.; Cleland, W. & Hussey, C. (1998) Electrochemical and spectroscopic characterization of self-assembled monolayers of ferrocenylalkyl compounds with amide linkages. *Langmuir* Vol.,14, No. 1, (Jan, 1998) 124-136, 0743-7463.

Sidorenko, A.; Ahn, H.; Kim, D.; Yang, H. & Tsukruk, V. (2002) Wear stability of polymer nanocomposite coatings with trilayer architecture. *Wear,* Vol. 252, No, 11-12, (Jun, 2002) 946-955, 0043-1648.

Sakata, H.; Kobayashi, M.; Otsuka, H. & Takahara, A. (2005) Tribological properties of poly(methyl methacrylate) brushes prepared by surface-initiated atom transfer radical polymerization. *Polymer Journal,* Vol. 37, No. 10, (Oct, 2005) 767-775, 0032-3896.

Song, S.; Ren, S.; Wang, J.; Yang, S.; Zhang, J. (2006) Preparation and tribological study of a peptide-containing alkylsiloxane monolayer on silicon. *Langmuir,* Vol. 22, No. 14, (Jun. 2006) 6010-6015, 0743-7463.

a, Song, S.; Zhou, J.; Qu, M.; Yang, S.; Zhang, J. (2008) Preparation and tribological behaviors of an amide-containing stratified self-assembled monolayers on silicon surface. *Langmuir,* Vol. 24, No. 1, (Jan. 2008) 105-109, 0743-7463.

b, Song, S.; Chu, R.; Zhou, J.; Yang, S.; Zhang, J. Y. (2008) Formation and tribology study of amide-containing stratified self-assembled monolayers: influences on the

underlayer structure. *The Journal of Physical Chemistry C,* Vol. 112, No, 10, (Feb, 2008) 3805-3810, 1932-7447.

Tao, Y. (1993) Structural comparison of self-assembled monolayers of n-alkanoic acids on the surfaces of silver, copper, and aluminum. *Journal of the American Chemical Society.* Vol. 115, No. 10, (May, 1993) 4350-4358, 0002-7863.

Tam-Chang, S.; Biebuyck, H.; Whitesides, G.; Jeon, N. & Nuzzo, R. (1995) Self-assembled monolayers on gold generated from alkanethiols with the structure $RNHCOCH_2SH$. *Langmuir*, Vol. 11, No. 11, (Nov, 1995) 4371-4382, 0743-7463.

a, Tsukruk, V.; Everson, M.; Lander, L. & Brittain, W. (1996) Nanotribological properties of composite molecular films: C60 anchored to a self-assembled monolayer. *Langmuir*, Vol. 12, No. 16, (Aug, 1996) 3905-3911, 0743-7463.

b, Tsukruk, V.; Bliznyuk, V.; Hazel, J.; Visser, D. & Everson, M. Organic molecular films under shear forces: Fluid and solid Langmuir monolayers. *Langmuir*, Vol. 12, No. 20 (Oct, 1996) 4840-4849, 0743-7463.

Tsukruk, V. & Blivnyuk, V. (1998) Adhesive and friction forces between chemically modified silicon and silicon nitride surfaces. *Langmuir*, Vol. 14, No. 2, (Jan, 1998) 446-455, 0743-7463.

Tsukruk, V.; Luzinov, I. & Julthongpiput, D. (1999) Sticky molecular surfaces: Epoxysilane self-assembled monolayers. *Langmuir,* Vol. 15, No. 9, (Apr, 1999) 3029-3032, 0743-7463.

Tsukruk, V. (2001) Molecular lubricants and glues for micro- and nanodevices. *Advanced Materials,* Vol. 13, No. 2, (Jan, 2001) 95-108, 0935-9648.

Ulman, A. (1996) Formation and structure of self-assembled monolayers. *Chemical Reviews,* Vol. 96, No. 4, (Jun, 1996), 1533-1554, 0009-2665.

Wong, S.; Takano, H. & Porter, M. (1998) Mapping orientation differences of terminal functional groups by friction force microscopy. *Analytical Chemistry,* Vol. 70, No. 24, (Dec, 1998) 5209-5212, 0003-2700.

Wang, X.; Tsui, O. & Xiao, X. (2002) Dynamic study of polymer films by friction force microscopy with continuously varying load. *Langmuir,* Vol. 18, No. 18, (Sep, 2002) 7066-7072, 0743-7463.

Wang, J.; Yang, S.; Liu, X.; Ren, S.; Guan, F. & Chen, M. (2004) Preparation and characterization of ZrO_2 thin film on sulfonated self-assembled monolayer of 3-mercaptopropyl trimethoxysilane. *Applied Surface Science,* Vol. 221, No. 1-4, (Jan, 2004) 272-280, 0169-4332.

Wang, J.; Liu, X.; Ren, S.; Guan, F. & Yang, S. (2005) Mechanical properties and tribological behavior of ZrO_2 thin films deposited on sulfonated self-assembled monolayer of 3-mercaptopropyl trimethoxysilane. *Tribology Letters,* Vol. 18, No. 4, (Apr, 2005) 429-436, 1023-8883.

Wang, M.; Liechti, K. M.; Wang, Q. & White, J. (2005) Self-assembled silane monolayers: Fabrication with nanoscale uniformity. *Langmuir,* Vol. 21, No. 5, (Mar, 2005) 1848-1857, 0743-7463.

Xiao, X.; Hu, J.; Charych, D. & Salmeron, M. (1996) Chain length dependence of the frictional properties of alkylsilane molecules self-assembled on Mica studied by atomic force microscopy. *Langmuir,* Vol. 12, No. 2, (Jan, 1996) 235-237, 0743-7463.

Xiao, X. & Qian L. (2000) Investigation of humidity-dependent capillary force. *Langmuir,* Vol. 16, No. 21, (Sep. 2000) 8153-8158, 0743-7463.

Zhao, B. & Brittain, W. (2000) Polymer brushes: surface-immobilized macromolecules. *Progress in Polymer Science.* Vol. 25, No. 5, (Jun, 2000) 677-710, 0079-6700.

Zhou, F.; Liu, W.; Chen, M. & Sun, D. (2001) A novel way to prepare ultra-thin polymer films through surface radical chain-transfer reaction. *Chemmical Commununications,* Vol. 23, (Dec, 2001) 2446-2447, 1359-7345.

Zhang, L.; Li, L.; Chen, S. & Jiang, S. (2002) Measurements of friction and adhesion for alkyl monolayers on Si(111) by scanning force microscopy. *Langmuir,* Vol. 18, No. 14, (Jul, 2002) 5448-5456, 0743-7463.

Zhang, Q. & Archer, L. (2003) Boundary lubrication and surface mobility of mixed alkylsilane self-assembled monolayers. *The Journal of Physical Chemistry B,* Vol. 107, No. 47, (Nov, 2003) 13123-13132, 1520-6106.

Zhang, Q. & Archer, L. (2005) Interfacial friction of surfaces grafted with one- and two-component self-assembled monolayers. *Langmuir,* Vol. 21, No.12, (Jun, 2005) 5405-5413, 0743-7463.

Zhang, G.; Howe, J.; Coffey, D. & Blom, D. (2006) A biomimetic approach to the deposition of ZrO_2 films on self-assembled nanoscale templates. *Materials Science and Engineering C: Biomimetic and Supramolecular Systems.* Vol. 26, No. 8, (Sep, 2006), 1344-1350, 0928-4931.

Zhao, J. Chen, M. An, Y. Liu, J. & Yan, F. (2008) Preparation of polystyrene brush film by radical chain-transfer polymerization and micromechanical properties, *Applied Surface Sciences.* Vol. 255, No. 5, (Dec, 2008) 2295-2302, 0169-4332.

Zlotnikov, I.; Gotman, I. & Gutmanas, E. (2008) Characterization and nanoindentation testing of thin ZrO_2 films synthesized using layer-by-layer (LbL) deposited organic templates. *Applied Surface Science,* Vol. 255, No. 5, (Dec, 2008) 3447-3453, 0169-4332.

Zhao, J.; Chen, M.; Liu, J.; Yan, F. (2009) Preparation and tribological studies of self-assembled triple-layer films. *Thin Solid Films,* Vol. 517, No. 13, (May, 2009) 3752-3759, 0040-6090.

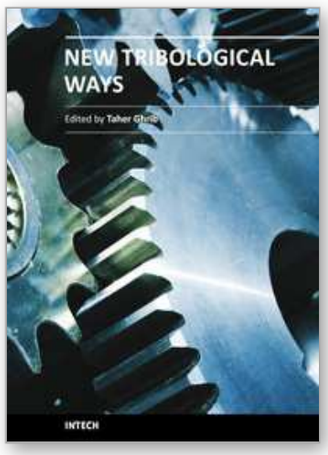

New Tribological Ways

Edited by Dr. Taher Ghrib

ISBN 978-953-307-206-7
Hard cover, 498 pages
Publisher InTech
Published online 26, April, 2011
Published in print edition April, 2011

This book aims to recapitulate old information's available and brings new information's that are with the fashion research on an atomic and nanometric scale in various fields by introducing several mathematical models to measure some parameters characterizing metals like the hydrodynamic elasticity coefficient, hardness, lubricant viscosity, viscosity coefficient, tensile strength .... It uses new measurement techniques very developed and nondestructive. Its principal distinctions of the other books, that it brings practical manners to model and to optimize the cutting process using various parameters and different techniques, namely, using water of high-velocity stream, tool with different form and radius, the cutting temperature effect, that can be measured with sufficient accuracy not only at a research lab and also with a theoretical forecast. This book aspire to minimize and eliminate the losses resulting from surfaces friction and wear which leads to a greater machining efficiency and to a better execution, fewer breakdowns and a significant saving. A great part is devoted to lubrication, of which the goal is to find the famous techniques using solid and liquid lubricant films applied for giving super low friction coefficients and improving the lubricant properties on surfaces.

InTech Europe
University Campus STeP Ri
Slavka Krautzeka 83/A
51000 Rijeka, Croatia
Phone: +385 (51) 770 447
Fax: +385 (51) 686 166
www.intechopen.com

InTech China
Unit 405, Office Block, Hotel Equatorial Shanghai
No.65, Yan An Road (West), Shanghai, 200040, China
中国上海市延安西路65号上海国际贵都大饭店办公楼405单元
Phone: +86-21-62489820
Fax: +86-21-62489821

IntechOpen